Laser-Induced Fluorescence Detection of Hot Molecular Oxygen in Flames Using an Alexandrite Laser

Kiefer, Johannes; Zhou, Bo; Zetterberg, Johan; Li, Zhongshan; Aldén, Marcus

Published in:
Applied Spectroscopy

DOI:
10.1366/14-07512

2014

Laser-Induced Fluorescence Detection of Hot Molecular Oxygen in Flames Using an Alexandrite Laser

Johannes Kiefer,[a,b,*,†] Bo Zhou,[c] Johan Zetterberg,[c] Zhongshan Li,[c] Marcus Alden[c]

[a] *School of Engineering, University of Aberdeen, Fraser Noble Building, Aberdeen AB24 3UE Scotland, UK*
[b] *Erlangen Graduate School in Advanced Optical Technologies, Universität Erlangen-Nürnberg, Paul-Gordan-Strasse 6, 91052 Erlangen, Germany*
[c] *Division of Combustion Physics, Lund University, P.O. Box 118, 22100 Lund, Sweden*

The use of an alexandrite laser for laser-induced fluorescence (LIF) spectroscopy and imaging of molecular oxygen in thermally excited vibrational states is demonstrated. The laser radiation after the third harmonic generation was used to excite the B–X (0-7) band at 257 nm in the Schumann–Runge system of oxygen. LIF emission was detected between 270 and 380 nm, revealing distinct bands of the transitions from B(0) to highly excited vibrational states in the electronic ground state, X ($v > 7$). At higher spectral resolution, these bands reveal the common P- and R-branch line splitting. Eventually, the proposed LIF approach was used for single-shot imaging of the two-dimensional distribution of hot oxygen molecules in flames.

Index Headings: **Schumann–Runge; Oxygen; Ultraviolet; Planar laser-induced fluorescence; PLIF.**

INTRODUCTION

Molecular oxygen is important in many areas, including the life sciences and the energy sector. Hot oxygen, i.e., oxygen in excited vibrational and electronic states, is of particular interest, for instance, in plasma physics,[1] where it is generated when oxygen atoms recombine or an oxygen molecule collides with an electron,[2] in atmospheric chemistry,[3] where photolysis of ozone by ultraviolet (UV) radiation is a common mechanism to form excited oxygen in the stratosphere and mesosphere;[4] and in combustion technology, where excited oxygen molecules are used in plasma-assisted flames[5] and residual oxygen in the hot exhaust gas is a key parameter in judging the performance of a combustor.[6] This work is concerned with the latter area. In most technical combustors (cold) oxygen from air is the oxidizer reacting with the fuel to form products such as carbon dioxide and water. However, traces of hot oxygen are present even in the exhaust gas of fuel-rich combustion processes owing to the chemical reaction equilibrium. To study the chemistry in flames and to unravel the complex chemical mechanisms and equilibriums, sensitive detection of small amounts of highly excited oxygen is desirable.

Most existing techniques for detection of molecular oxygen either use indirect approaches, for example, the fluorescence of a tracer influenced by the presence of oxygen,[7] or they are based on vibrational ground or low-lying excited states of oxygen, hence the signal is always dominated by cold oxygen due to the higher population. In this context, the available methods include laser-induced fluorescence (LIF) using excitation at 193 or 226 nm;[8–13] vibrational and pure-rotational coherent anti-Stokes Raman scattering (CARS) spectroscopy;[14–17] and spontaneous Raman scattering.[18–22] Assuming thermal equilibrium, it is possible to determine the population of excited oxygen from a combined measurement of the ground state population and the temperature. However, this assumption can hardly be justified in the vicinity of the reaction zone in a flame where the complex chemistry produces nonequilibrium species such as radicals in electronically excited states. Therefore, a direct measurement of the species of interest is desirable.

For detecting traces of hot molecular oxygen in a combustion gas, LIF using selective electronic excitation of vibrationally excited molecules in the electronic ground state has proved its potential. The well-known $B^3\Sigma_u^- \leftarrow X^3\Sigma_g^-$ Schumann–Runge system exhibits strong absorption and emission bands in the UV and deep-UV spectrum.[23,24] Again, radiation at wavelengths around 193 or 226 nm can be used for this purpose.[8,13,25,26] The most common approach, however, is to excite the B–X (0-5), (1-6), or (2-7) bands around 248 nm and to detect fluorescence signals between 270 and 400 nm.[27–29] The major benefit of excitation at 248 nm is that conventional krypton fluoride excimer lasers can be used. They can provide high-energy pulses sufficiently short to resolve turbulent phenomena in flames. However, the beam profile characteristics and the limited tuning range may be disadvantageous in certain applications: The beam profile may prevent a sufficiently thin laser sheet to be formed, leading to limited spatial resolution, and the limited tuning range may prevent maximizing the signal and minimizing interferences. Alternatively, dye lasers can be used for O_2-LIF. To reach the wavelengths required, one can use either coumarin dyes pumped by UV lasers such as excimer lasers or third harmonic neodymium-doped yttrium aluminum garnet lasers (lasers delivering radiation of suitable wavelength after second harmonic generation or other types of frequency mixing).[30] Unfortunately, coumarin dyes are relatively unstable and toxic, and the frequency-conversion may be difficult due to inhomogeneous beam profiles and low pulse energy. Therefore, exhibiting high pulse energy and a close-to-Gaussian beam profile, the direct use of the radiation of a pulsed solid state laser would be

Received 3 March 2014; accepted 5 May 2014.
* Author to whom correspondence should be sent. E-mail: jkiefer@uni-bremen.de.
† Current address: Technische Thermodynamik, Universität Bremen, Badgasteiner Strasse 1, 28359 Bremen, Germany
DOI: 10.1366/14-07512

0003-7028/14/6811-1266/0

advantageous. Moreover, in certain flames, a slightly longer wavelength (compared with the conventional 248 nm) may be advantageous because lower photon energy means a lower probability of photodissociation of molecular species. This may influence the local flame chemistry, or it may generate species that can potentially emit interfering fluorescence signals. An example of such interference from photodissociated molecules was recently investigated for planar laser-induced fluorescence (PLIF) of the formyl radical.[31]

Tuneable over a wide spectral range, alexandrite lasers have great potential in the area of laser diagnostics.[32–34] In particular, we have demonstrated the feasibility of using multimode alexandrite lasers for LIF applications, e.g., to visualize methylidyne (CH) and HCO radicals.[35–38] A key feature of using multimode radiation can be the simultaneous excitation of several rotational transitions, hence improving the signal-to-noise ratio (S/N).[37] However, care must be taken when the wavelength is selected as the spectral bandwidth may lead to excitation of unwanted species, resulting in spectral interferences.[31,39] In contrast, in single-longitudinal-mode operation, alexandrite lasers allow individual rotational transitions to be excited, hence obtaining high-resolution spectra as well as avoiding spectral interferences from other species exhibiting absorption lines in the vicinity of the species of interest.[33,40] Herein, the multimode option is used. Another beneficial characteristic of the alexandrite laser is its long pulse duration (70–120 ns) compared with conventional pulsed (Q-switched) lasers (a few nanoseconds). In a LIF application, this allows each molecule to contribute to the signal several times as the typical lifetimes in the excited state are on the order of a few nanoseconds so that an individual molecule can be excited and fluoresce repeatedly during a single pulse. In the case of oxygen, the relaxation times may significantly vary with the vibrational states involved and the local collisional partners.[41,42] This needs to be taken into account should quantitative measurements be the aim. In our application, where highly excited vibrational states of oxygen are involved in the LIF process, the signal enhancement via cycling during a single laser pulse is rather limited as vibrational energy transfer between these states can be on the order of microseconds or even longer.[43,44]

In this work, we demonstrate the use of a pulsed alexandrite laser for laser-induced fluorescence of vibrationally excited molecular oxygen. Moreover, this study represents the first attempt of using excitation in the (0-7) Schumann–Runge band at 257 nm for oxygen LIF detection. Spectrally resolved LIF measurements were carried out to understand and confirm the origin of the signals, and the developed method was then applied to visualizing the two-dimensional distribution of hot oxygen in two different flames using single-shot PLIF.

EXPERIMENTAL

A pulsed, tunable, and multimode alexandrite laser (model 101PAL, Light Age Inc.) was used as the light source for the LIF experiments. In contrast to previous work[33,35–37] where a ring-cavity alexandrite laser was used, the present system has a linear cavity that is easier to operate and hence simplifies the experiment. The laser is tunable from 720 to 785 nm, delivering nearly constant pulse energy of 250 mJ. The fundamental output was frequency tripled through second and third harmonic generation in β-barium borate crystals, delivering radiation at around 257 nm ($\sim$2.25 cm^{-1} line width, $\sim$70 ns pulse duration, $\sim$14 mJ pulse energy) for oxygen excitation. The third harmonic radiation was separated through a Pellin–Broca prism and guided through some optical components to the center of a burner. The laser wavelength was monitored by directing part of the fundamental beam to a wavemeter (WS/6-200, HighFinesse).

Two types of experiment were carried out. To ensure that oxygen molecules were detected exclusively, the laser-induced emission was spectroscopically analyzed along a one-dimensional (1D) line perpendicularly across the reaction zone of a laminar flame using an imaging spectrograph (focal length 500 mm, grating 150 grooves/mm, slit width 50 μm) equipped with an intensified charge-coupled device (CCD) camera. In the spectroscopic measurements, a 200 mm cylindrical lens was used to form a 3 mm high laser sheet passing the flame center axis 3 mm above the burner exit. The laser-induced emission was collected in a direction perpendicular to the laser beam using a 100 mm lens with a diameter of 5.08 cm (2 in.). A color glass filter (Schott WG280, 3 mm thick) was mounted in front of the slit to block elastically scattered laser light. The spectra were averaged over 3000 shots and had a spectral resolution of $\sim$2.5 nm. The second experiment aimed at visualizing the two-dimensional distribution of hot molecular oxygen in flames. For this purpose, a 30 mm high and 100 μm thick laser sheet was formed using two cylindrical lenses of −40 and 200 mm focal length. The LIF signal generated in the laser sheet was imaged using an intensified CCD camera (1024 × 1024 pixels of 12.8 μm) equipped with a UV objective. A combination of two color glass filters (UG5 and WG295, 3 mm thick each) was used to block elastically scattered light and other spectral interferences.

Measurements were performed in methane/oxygen flames stabilized on a welding torch burner with a nozzle diameter of 1.8 mm. A lean flame (equivalence ratio $\varphi = 0.9$) and a rich flame ($\varphi = 1.47$) were established with total flow rates of 5.13 and 7.18 liters/min, respectively (Reynolds numbers 3690 and 5100).

To support the spectroscopic investigations, spectral simulations were carried out using the LIFSim software.[45] LIFSim is a software tool that allows oxygen B–X absorption and LIF spectra (excitation and emission) to be simulated. LIF signals are calculated using a three-level non-transient linear model.[45]

RESULTS AND DISCUSSION

Spectroscopy. To find a suitable excitation wavelength, the spectrum between 256 and 260 nm was considered, and test measurements revealed that the region around 257 nm is best suited. Figure 1 displays a simulated absorption spectrum of oxygen. The simulation reveals several absorption features within the 1 nm spectral range around 257 nm. A wavelength of

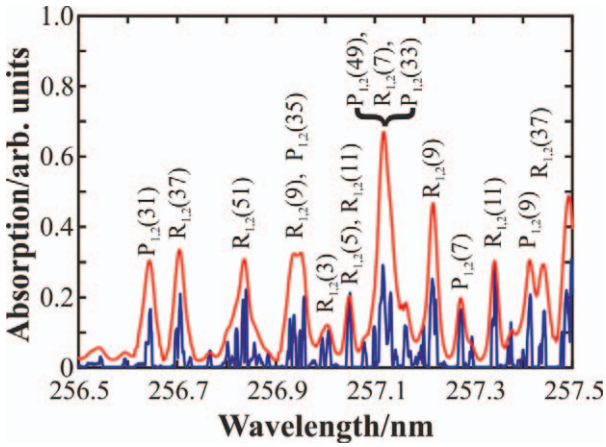

FIG. 1. Absorption spectrum of O_2 simulated using LIFSim and rotational assignment of lines. Conditions for calculation: 3000 K, 1 bar, resolution 2.25 cm^{-1}; the blue line shows the corresponding high-resolution spectrum.

256.972 nm was identified as the best compromise for obtaining a sufficient S/N from oxygen LIF and simultaneously minimizing interference from other species. For example, formyl (HCO) and hydroxyl (OH) radicals, as well as polycyclic aromatic hydrocarbons (PAHs), exhibit absorption lines in this spectral region, too (further emission spectra recorded with varied excitation wavelengths can be found together with a detailed discussion of potential interferences in Zhou et al.[31]). The chosen wavelength of 256.972 nm means excitation in an absorption band where the $R_1(9)$, $R_2(9)$, $P_1(35)$, and $P_2(35)$ lines overlap. The individual lines can be observed in the high-resolution spectrum displayed. However, it should be noted that the optimal wavelength determined in our experiment does not coincide with a peak maximum in the simulated spectrum. This may indicate that the available spectroscopic constants of the highly excited vibrational states involved in our LIF approach are not perfectly accurate.

The spectrally resolved laser-induced emission recorded along a 1D line in the lean methane/oxygen flame is displayed in Fig. 2. The radial position at 0 mm

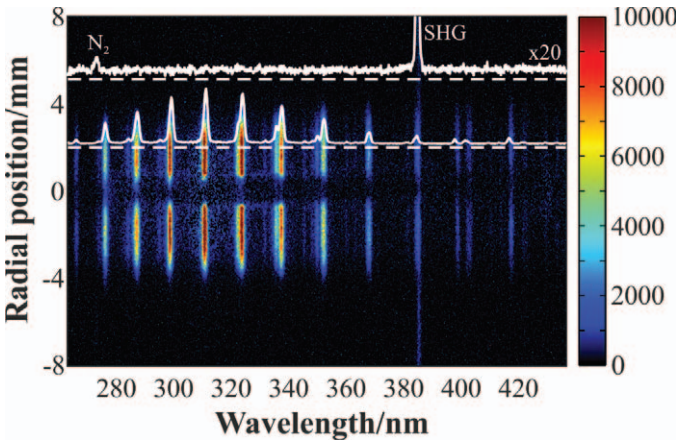

FIG. 2. Spectrally resolved emission along a 1D line across the reaction zone of a laminar lean methane/oxygen flame and spectra extracted at selected radial positions indicated by dashed lines. The laser wavelength was 256.972 nm.

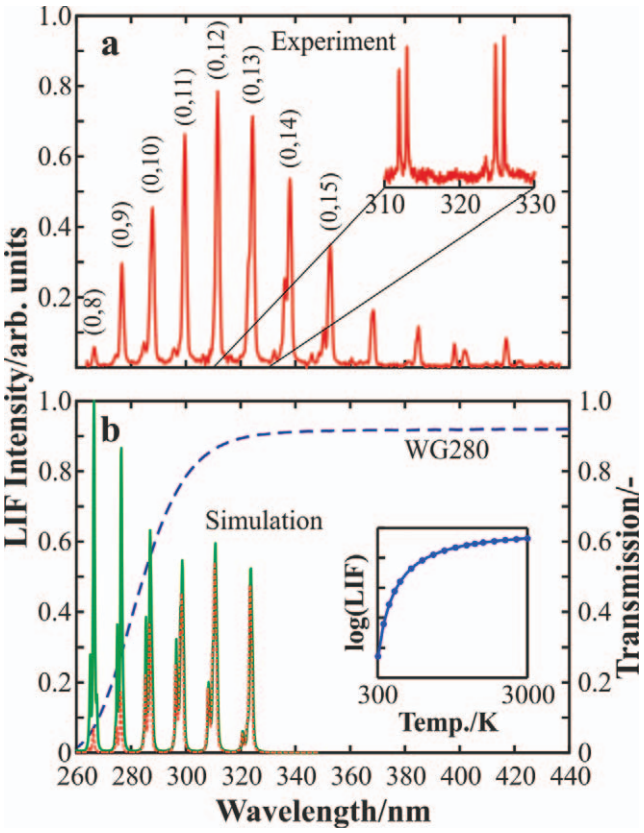

FIG. 3. Emission spectrum of O_2. (**a**) Experimental LIF data; the inset displays the spectral region 310–330 nm recorded with high resolution; the laser wavelength was 256.972 nm. (**b**) Simulated LIF data using LIFSim (green solid line; note that states higher than $v = 14$ are not implemented), the transmission curve of the WG280 color glass filter (blue dashed line), and a convolution of the spectrum and the filter function (red dashed line); the inset displays the temperature dependence of the LIF signal. Conditions for calculation: 3000 K, 1 bar, resolution 0.2 nm.

represents the center axis of the burner, where only weak signals can be found (we note that these signals mainly originate from O_2-LIF and appear in the image due to the slightly unsteady behavior of the flame and the averaging when the data were collected). The spectra extracted at the radial positions indicated by the dashed lines are plotted in the Fig. 2 as well. At the 2 mm radial position, a regular pattern of emission lines can be observed. At larger distances from the center, i.e., radial positions >4 mm, a weak Raman signal of nitrogen can be identified as well as a strong line at ~388 nm. The latter line can be attributed to straylight of the second harmonic laser radiation, which could not be fully separated from the third harmonic by the Pellin–Broca prism.

The experimental LIF emission spectrum from Fig. 2 (2 mm radial position) is shown in greater detail in Fig. 3a. Distinct lines can be observed between 260 and 430 nm after an envelope distribution as a result of the spectral transmission of the WG280 filter. Figure 3b shows the simulated emission spectrum together with the filter transmission curve. It becomes clear that the strongest lines in the emission spectrum appear in the short wavelength region, but they are reduced in intensity by the filter. A convolution of the simulated

spectrum and the filter transmission function is shown as red dashed line in Fig. 3b. It agrees well with the experimental spectrum in the corresponding spectral range.

The individual peaks can be assigned to different Schumann–Runge bands of oxygen. Excitation was predominantly made in the B–X (0-7) band. This means that fluorescence emission predominantly takes place originating from the B(0) state. A couple of weak and slightly shifted bands appear as a result of fluorescence from B(1) and B(2) states after excitation of a small amount of molecules in B–X (1-8) and (2-9) bands. The simulated spectrum indicates that the peaks in the experimental spectrum represent overlapping signals from multiple rotational transitions. To confirm the fine structure, the 150 grooves/mm grating in the spectrograph was replaced by a 1200 grooves/mm grating to obtain higher spectral resolution. The inset in Fig. 3a plots the high-resolution emission spectrum between 310 and 330 nm, revealing the splitting into doublets of P- and R-branch lines.

The inset in Fig. 3b shows the dependence of the LIF signal on the temperature calculated from the thermal population of the initial X(7) state according to the Boltzmann distribution. Significant (detectable) LIF signals can be observed at temperatures above 1500 K, and the signal intensity increases by approximately two orders of magnitude between 1500 and 3000 K. This increase must be taken into account when aiming at quantitative measurements.

It was noted above that a variety of other flame species have absorption bands around 260 nm. The main candidates are OH, HCO, PAH, and formaldehyde. The latter can be photodissociated to form HCO. A detailed investigation of potential interferences that may result from selection of an inappropriate excitation wavelength can be found in Zhou et al.,[31] where the relevant spectral region was analyzed in the context of HCO PLIF. From the emission spectra analyzed in Fig. 2, we can conclude that a careful selection of the excitation wavelength and the use of appropriate spectral filters allow species-specific laser-induced fluorescence experiments to be carried out in lean premixed flames. However, in rich flames a large variety of additional species, e.g., PAHs, may be present, capable of absorbing the UV laser radiation and thus representing a potential means of interference. To investigate the possibility of performing hot oxygen-LIF in rich flames, experiments were carried out in a $\varphi = 1.47$ methane/oxygen flame.

Figure 4 shows the spectrally resolved laser-induced emission recorded along a 1D line in the rich flame using a laser wavelength of 256.972 nm, a wavelength that was found optimal for O_2-LIF. Due to the slightly unsteady flame and the time averaging, the center region contains significant signals from the flame front species. The spectrum extracted close to the center represents the flame front and reveals distinct peaks of hot oxygen, similar to the lean flame case. However, the oxygen peaks are now on top of a broad underlying fluorescence background originating predominantly from PAH. The strength of this PAH interference is in the same order of magnitude as the O_2-LIF signal. The rich flame chemistry is also evident in the enhanced CH signal at 430 nm that

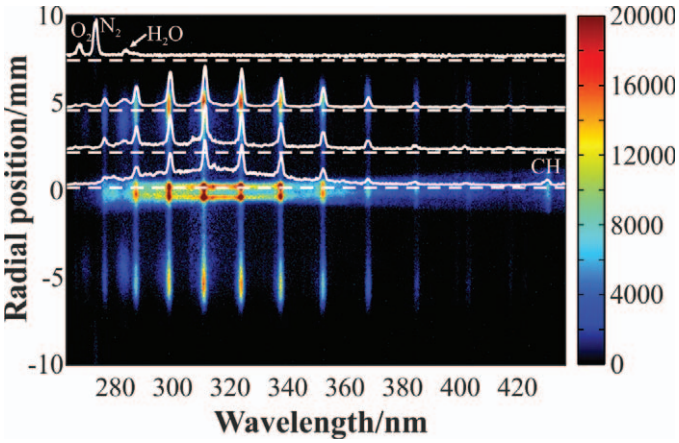

FIG. 4. Spectrally resolved emission along a 1D line inside a rich methane/oxygen flame and spectra extracted at selected radial positions indicated by dashed lines. The laser wavelength was 256.972 nm.

was not observable in the lean flame at this excitation wavelength. At the set wavelength, the second harmonic radiation is capable of exciting CH radicals at 385.458 nm where it can be absorbed by R-branch transitions in the hot CH A-X(2,1) band. At the 2 mm radial position, the oxygen signals dominate and the broad background is significantly reduced. As the flame is rich, these oxygen signals are due to the residual molecular oxygen not consumed in the flame front because of the chemical equilibrium. Further downstream, surrounding air is penetrating the flame and heated up in the secondary reaction zone; hence, the signal intensity is enhanced. PAH interferences are not observed at this position; however, two minor broadband emission features at 283 and 308 nm from OH radicals are present. Their contribution to the integrated amount of signal is small. At the 7.5 mm distance from the center axis, the Raman signals of the laboratory air molecules can be identified.

From the data illustrated in Fig. 4, we conclude that our O_2-LIF approach can in principle be applied to rich flames; however, care must be taken when the signals are interpreted as unspecific interferences from PAH overlap with the oxygen fluorescence. This is particularly the case in the primary reaction zone where a PAH contribution of about 50% (this value may vary significantly with stoichiometry) to the overall signal is found. Neither changing the wavelength nor spectral filtering allows this background to be suppressed.

In the following section, the developed method for LIF detection of hot molecular oxygen is used for visualizing the two-dimensional distribution of O_2 in flames.

Imaging. Figure 5 illustrates a series of five single-shot PLIF images recorded in the lean premixed methane/oxygen flame. Typical values of the S/N are in the order of 20–30. The flame was laminar; thus, only small differences between the individual images can be observed. In the center of the images, a cone without signal is visible directly above the burner nozzle exit. In this cone, the fresh unburned methane/oxygen mixture is present. Despite the high oxygen concentration, no LIF signals can be found as virtually no molecules occupy the $v = 7$ state at ambient temperature according to the

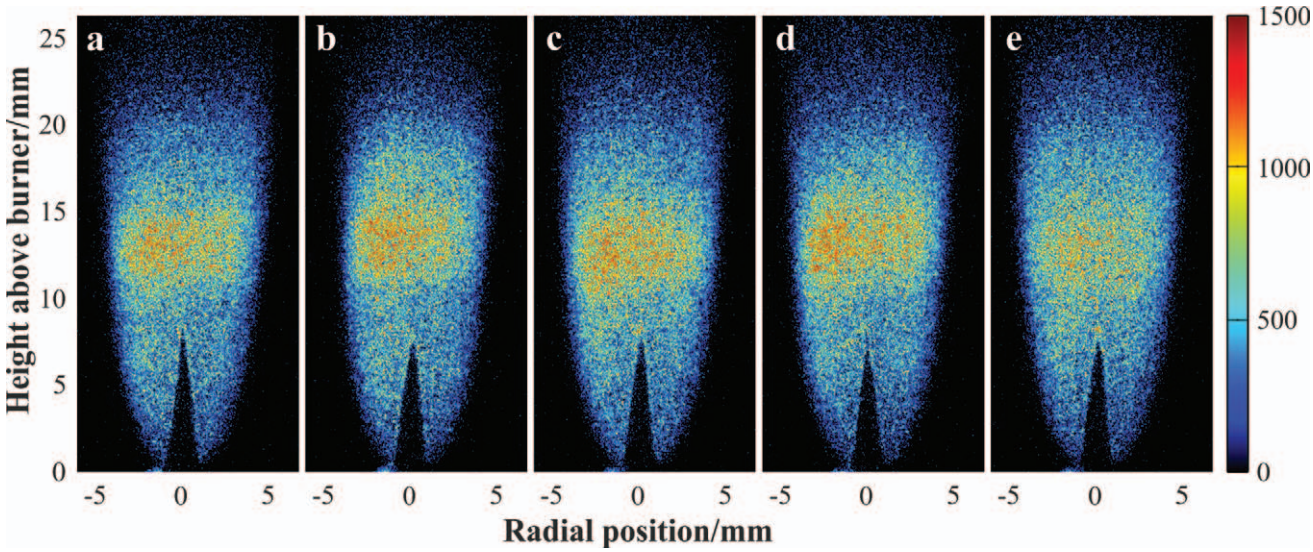

FIG. 5. Single-shot PLIF images of hot molecular oxygen recorded in a lean premixed flame.

Boltzmann distribution. In the reaction zone, the temperature increases (the adiabatic temperature of a $\varphi = 0.9$ methane/oxygen flame is ~3040 K), and hot oxygen molecules can be found in the flame front and a wide region of the post-combustion gas due to the excess oxygen. Note that the signal inhomogeneities with height above burner are mainly due to inhomogeneities in the laser sheet rather than to changes in the oxygen concentration or temperature. Between 5 and 20 mm height, the profile was close to a Gaussian distribution in vertical direction. The wings of the laser sheet, i.e., below 5 and above 20 mm, exhibit further inhomogeneities.

Figure 6 displays a series of five single-shot PLIF images recorded in the rich premixed methane/oxygen flame. Owing to the higher flow velocity and lower flame speed, the flame is not as stable as the flame discussed above and, as a consequence, the single-shot images reveal slightly wrinkled flame structures. Again a cone of cold, fresh gas can be identified at the nozzle exit of the welding torch. Strong signals can be observed in the primary flame front where the temperature increases due to the combustion process (the adiabatic temperature of a $\varphi = 1.47$ methane/oxygen flame is ~2990 K). Part of the oxygen supplied is heated before it is consumed. Hence, a thin layer is visible in the PLIF images. We note that a fraction of the signal in the order of 50% in this layer may be originating from PAH molecules. Downstream of the primary flame front, a very weak signal can be found. Although the methane/oxygen mixture is rich, a small amount of oxygen is present in this post-reaction gas owing to the chemical equilibrium. Further downstream, i.e., when oxygen from the surrounding air enters the flame via diffusion and is heated up, the signal intensity increases again, forming a secondary reaction zone where the remaining hydrocarbon molecules and other intermediates such as carbon monoxide and hydrogen are oxidized.

To confirm the presence and the qualitative profile of hot O_2 in the rich flame, a 1D simulation of the combustion chemistry across the initial reaction zone was carried out using CHEMKIN with the 1D free-propagation model and the GRI 3.0 mechanism.[46] The temperature profile, the overall oxygen mole fraction, and the resulting mole fraction of oxygen in the $v = 7$ state are plotted in Fig. 7, together with an experimental profile of the LIF signal recorded in the flame. The experimental data are extracted from the PLIF image in Fig. 6e (the exact position is indicated by the white line). The temperature at 0 mm radial position is room temperature and then quickly raises to beyond 3000 K in the reaction zone before it slightly decreases again and settles around 3000 K. The calculated oxygen mole fractions are plotted on a logarithmic scale to better visualize the features. The overall oxygen concentration is high in the premixed gas and rapidly decreases in the flame front as the temperature goes up. However, the oxygen is not fully consumed, and its mole fraction settles around 0.01. Using the Boltzmann distribution, the mole fraction of oxygen molecules occupying the $v = 7$ vibrational state is calculated from the total oxygen and the temperature. At room temperature, virtually no oxygen is in the $v = 7$ state. As the temperature increases, a significant amount of vibrationally excited oxygen is present, peaking in the reaction zone before it settles at a constant level around 10^{-5}. Despite significant noise in the experimental data, the behavior predicted in the simulation is in excellent agreement with the qualitative experimental O_2 profile that is also plotted on a logarithmic scale to allow a comparison. The contribution or interference from large hydrocarbons, which was identified in the spectrally resolved data, seems to have a minor impact on the qualitative distribution of hot oxygen but needs to be kept in mind when interpreting the results.

SUMMARY AND CONCLUSIONS

Herein, we have demonstrated the use of a pulsed multimode alexandrite laser for spectroscopy and imaging of hot molecular oxygen in flame environments. The laser output was frequency tripled to provide tuneable radiation at 257 nm suitable for excitation in the (0,7) band of the $B^3\Sigma_u^- \leftarrow X^3\Sigma_g^-$ Schumann–Runge system. Spectrally resolved measurements revealed

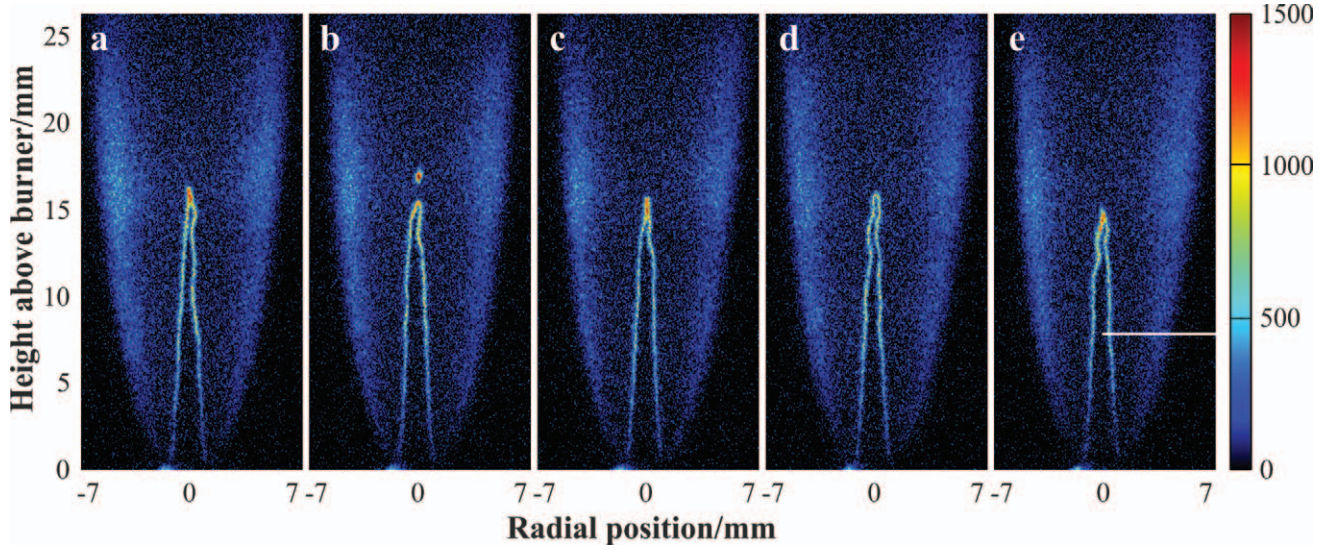

FIG. 6. Single-shot PLIF images of hot molecular oxygen recorded in a rich premixed flame. The line in (e) indicates where the profile shown in Fig. 7 was extracted.

that the signals originate from transitions between the B(0) state and highly excited vibrational levels in the electronic ground state. High-resolution spectra showed the typical line splitting of the oxygen P- and R-branch lines. The developed excitation-detection approach was then used in planar LIF imaging experiments for visualizing the distribution of hot oxygen in lean and rich methane/oxygen flames. An opportunity for improvement in future work will be to replace the longpass filter for suppression of elastically scattered light by a band-stop filter (e.g., notch). This will allow detecting not only fluorescence signals of B–X(0, $v > 7$) bands but also of B–X(0, $v < 7$) transitions, which are often stronger due to being less off-diagonal.

In conclusion, our method represents a straightforward approach for imaging hot molecular oxygen in flames. Owing to the high initial vibrational state, the signal originates exclusively from high temperature (>1500 K) oxygen, and signals from cold regions of the flame are not detected at all. However, a disadvantage arising from this point is that because of the small fraction of molecules occupying the X(7) state according to the Boltzmann distribution, the total concentration of oxygen needs to be in the order of 1%. This limits the applicability to high-temperature flames, e.g., when hydrogen is combusted or hydrocarbons are converted with oxygen rather than air. To get an idea for the flame types and conditions under which the PLIF method can

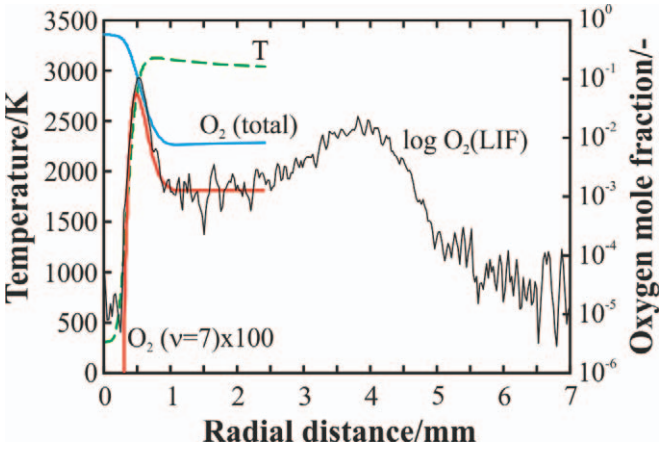

FIG. 7. Temperature and oxygen profiles simulated with CHEMKIN together with the measured qualitative oxygen profile.

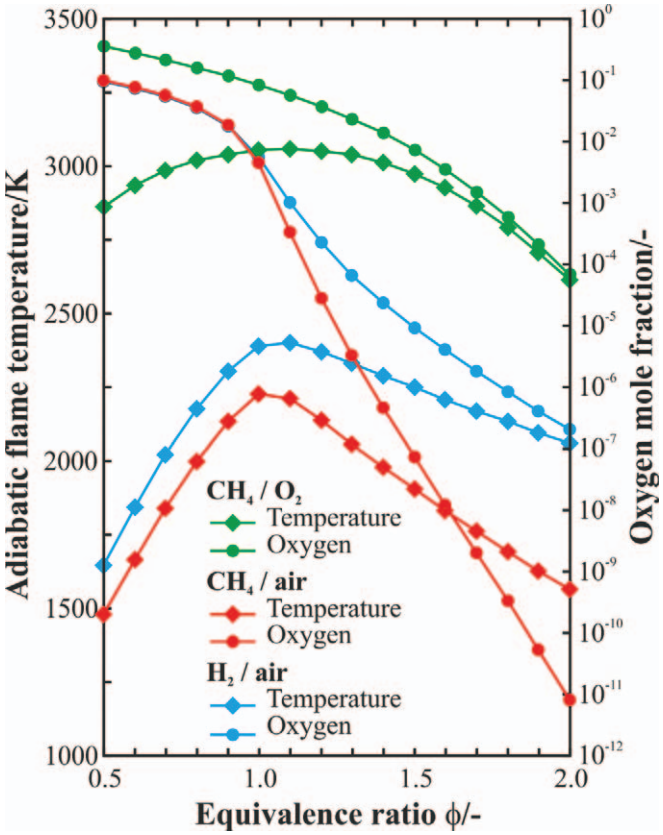

FIG. 8. Adiabatic flame temperature and oxygen mole fraction at thermodynamic equilibrium after isobaric combustion as function of equivalence ratio.

be used, Fig. 8 displays adiabatic flame temperatures and post-combustion molar oxygen concentrations as a function of stoichiometric ratio for methane/air, methane/oxygen, and hydrogen/air flames. The data were calculated from a free Gibbs energy minimization for constant pressure combustion taking into account 24 chemical species (reactants, products, and intermediates) for the methane flames and seven species for the hydrogen case. The initial temperature was set 300 K and the pressure was 1 atm. It becomes clear that the required flame temperature is reached in all flames for the stoichiometries considered, i.e., $0.5 < \varphi < 2.0$. Regarding the required oxygen concentration, however, the range $0.5 < \varphi < 1.0$ for the air-fed methane and hydrogen flames and the range $0.5 < \varphi < 1.5$ for methane/oxygen flames is feasible.

Capable of single-shot imaging, the hot-O_2 PLIF will be of particular interest for studying turbulent lean and stoichiometric premixed flames that are relevant, e.g., in the development of gas turbine burners. In rich flames, care must be taken as interference from PAHs may occur and bias the interpretation of the data. The relatively wide tunability of the alexandrite laser we used may also facilitate O_2-based temperature field measurements by two-line LIF in the future. However, care must be taken when suitable lines are selected to avoid interference from other species.

ACKNOWLEDGMENTS

This work was financed by the Swedish Energy Agency through Centre for Combustion Science and Technology (CECOST), the Swedish-Chinese collaboration (Project 33305-1), Vetenskapsrådet (VR (Swedish Research Council)), and the European Research Council Advanced Grant DALDECS. JK gratefully acknowledges support from the European Union through the LASERLAB-EUROPE (Lund Laser Centre) and from the Scottish Funding Council (SFC) through the Scottish Sensor Systems Centre (SSSC).

1. C. Küllig, K. Dittmann, T. Wegner, I. Sheykin, K. Matyash, D. Loffhagen, R. Schneider, J. Meichsner. "Dynamics and Electronegativity of Oxygen RF Plasmas". Contrib. Plasma Phys. 2012. 52(10): 836-846.
2. N.L. Aleksandrov, E.M. Anokhin. "Low-Energy Electron Attachment and Detachment In Vibrationally Excited Oxygen". J. Phys. D. 2009. 42(22): 225210.
3. R. Toumi, B.J. Kerridge, J.A. Pyle. "Highly Vibrationally Excited Oxygen as a Potential Source of Ozone in the Upper-Stratosphere and Mesosphere". Nature. 1991. 351(6323): 217-219.
4. Y. Matsumi, M. Kawasaki. "Photolysis of Atmospheric Ozone in the Ultraviolet Region". Chem. Rev. 2003. 103(12): 4767-4782.
5. V.V. Smirnov, O.M. Stelmakh, V.I. Fabelinsky, D.N. Kozlov, A.M. Starik, N.S. Titova. "On the Influence of Electronically Excited Oxygen Molecules on Combustion of Hydrogen-Oxygen Mixture". J. Phys. D. 2008. 41(19): 192001.
6. N. Collings, J.A. Harris, K. Glover. "Estimating IC Engine Exhaust Gas Lambda and Oxygen from the Response of a Universal Exhaust Gas Oxygen Sensor". Meas. Sci. Technol. 2013. 24(9): 095101.
7. K. Mohri, M. Luong, G. Vanhove, T. Dreier, C. Schulz. "Imaging of the Oxygen Distribution in an Isothermal Turbulent Free Jet Using Two-Color Toluene LIF Imaging". Appl. Phys. B. 2011. 103(3): 707-715.
8. A. Cessou, P. Colin, D. Stepowski. "Statistical Investigation of the Turbulent Flame Geometrical Structures in a Liquid Oxygen/Gaseous Hydrogen Shear-Coaxial Jet". Proc. Combust. Inst. 1998. 27(1): 1039-1045.
9. G.A. Massey, C.J. Lemon. "Feasibility of Measuring Temperature and Density Fluctuations in Air Using Laser-Induced O_2 Fluorescence". IEEE J. Quant. Electronics. 1984. QE-20: 454-457.
10. G. Laufer, R.L. McKenzie, D.G. Fletcher. "Method for Measuring Temperatures and Densities in Hypersonic Wind Tunnel Air Flows Using Laser-Induced O_2 Fluorescence". Appl. Opt. 1990. 29(33): 4873-4883.
11. R.B. Miles, W.R. Lempert. "Quantitative Flow Visualization in Unseeded Flows". Ann. Rev. Fluid Mech. 1997. 29: 285-326.
12. M.P. Lee, P.H. Paul, R.K. Hanson. "Quantitative Imaging of Temperature Fields in Air Using Planar Laser-Induced Fluorescence of O_2". Opt. Lett. 1987. 12(2): 75-77.
13. M.D. Di Rosa, K.G. Klavuhn, R.K. Hanson. "LIF Spectroscopy of NO and O_2 in High-Pressure Flames". Combust. Sci. Technol. 1996. 118(4-6): 257-283.
14. F. Beyrau, A. Datta, T. Seeger, A. Leipertz. "Dual-Pump CARS for the Simultaneous Detection of N_2, O_2 and CO in CH_4 Flames". J. Raman Spectrosc. 2002. 33(11-12): 919-924.
15. L. Martinsson, P.-E. Bengtsson, M. Aldén. "Oxygen Concentration and Temperature Measurements in N_2-O_2 Mixtures Using Rotational Coherent Anti-Stokes Raman Spectroscopy". Appl. Phys. B. 1996. 62(1): 29-37.
16. S. Roy, J.R. Gord, A.K. Patnaik. "Recent Advances in Coherent Anti-Stokes Raman Scattering Spectroscopy: Fundamental Developments and Applications in Reacting Flows". Prog. Energy Combust. Sci. 2010. 36(2): 280-306.
17. T. Seeger, J. Kiefer, Y. Gao, B.D. Patterson, C.J. Kliewer, T.B. Settersten. "Suppression of Raman-Resonant Interferences in Rotational Coherent Anti-Stokes Raman Spectroscopy Using Time-Delayed Picosecond Probe Pulses". Opt. Lett. 2010. 35(12): 2040-2042.
18. O. Keck, W. Meier, W. Stricker, M. Aigner. "Establishment of a Confined Swirling Natural Gas/Air Flame as a Standard Flame: Temperature and Species Distributions from Laser Raman Measurements". Combust. Sci. Technol. 2002. 174(8): 117-151.
19. M.C. Weikl, F. Beyrau, J. Kiefer, T. Seeger, A. Leipertz. "Combined Coherent Anti-Stokes Raman Spectroscopy and Linear Raman Spectroscopy for Simultaneous Temperature and Multiple Species Measurements". Opt. Lett. 2006. 31(12): 1908-1910.
20. Q.V. Nguyen, R.W. Dibble, C.D. Carter, G.J. Fiechtner, R.S. Barlow. "Raman-LIF Measurements of Temperature, Major Species, OH, and NO in a Methane-Air Bunsen Flame". Combust. Flame. 1996. 105(4): 499-510.
21. P.A. Nooren, M. Versluis, T.H. van der Meer, R.S. Barlow, J.H. Frank. "Raman-Rayleigh-LIF Measurements of Temperature and Species Concentrations in the Delft Piloted Turbulent Jet Diffusion Flame". Appl. Phys. B. 2000. 71(1): 95-111.
22. A.R. Masri, R.W. Dibble, R.S. Barlow. "The Structure of Turbulent Nonpremixed Flames Revealed by Raman-Rayleigh-LIF Measurements". Prog. Energy Combust. Sci. 1996. 22(4): 307-362.
23. M.W. Feast. "The Schumann-Runge O_2 Emission Bands in the Region 3100A–2500A". Proc. Phys. Soc. 1950. 63(6): 549-556.
24. M. Ackerman, F. Biaume. "Structure of the Schumann-Runge Bands from 0-0 to 13-0 Band". J. Mol. Spectrosc. 1970. 35(1): 73-82.
25. B.L. Upschulte, M.G. Allen, K.R. McManus. "Fluorescence Imaging of NO and O_2 in a Spray Flame Combustor at Elevated Pressures". Proc. Combust. Inst. 1996. 27(2): 2779-2786.
26. J.E.M. Goldsmith, R.J.M. Anderson. "Laser-induced Fluorescence Spectroscopy and Imaging of Molecular Oxygen in Flames". Opt. Lett. 1986. 11(2): 67-69.
27. A. Arnold, W. Ketterle, H. Becker, J. Wolfrum. "Simultaneous Single-Shot Imaging of OH and O_2 Using a Two-Wavelength Excimer Laser". Appl. Phys. B. 1990. 51(2): 99-102.
28. P. Andresen, A. Bath, W. Gröger, H.W. Lülf, G. Meijer, J.J. ter Meulen. "Laser-Induced Fluorescence with Tunable Excimer Lasers as a Possible Method for Instantaneous Temperature Field Measurements at High Pressure: Checks with an Atmospherics Flame". Appl. Opt. 1988. 27(2): 365-378.
29. H. Neij, M. Alden. "Application of Two-Photon Laser-Induced Fluorescence for Visualization of Water Vapor in Combustion Environments". Appl. Opt. 1994. 33(27): 6514-6523.
30. B.R. Lewis, S.T. Gibson, K.G.H. Baldwin, P.M. Dooley, K. Waring. "Comparative Very-High-Resolution VUV Spectroscopy: Laser Spectroscopy of O_2". Surf. Rev. Lett. 2002. 9(1): 31-38.
31. B. Zhou, J. Kiefer, J. Zetterberg, Z.S. Li, M. Aldén. "Strategy for PLIF Single-Shot HCO Imaging in Turbulent Hydrocarbon Flames". Combust. Flame. 2014. 161(6): 1566-1574.
32. Z.S. Li, M. Afzelius, J. Zetterberg, M. Aldén. "Applications of a Single-Longitudinal-Mode Alexandrite Laser for Diagnostics of Parameters of Combustion Interest". Rev. Sci. Instrum. 2004. 75(10): 3208-3215.

33. J. Kiefer, Z.S. Li, J. Zetterberg, M. Linvin, M. Aldén. "Simultaneous Laser-Induced Fluorescence and Sub-Doppler Polarization Spectroscopy of the CH Radical". Opt. Commun. 2007. 270(2): 347-352.
34. J. Zetterberg, Z.S. Li, M. Afzelius, M. Aldén. "Two-Dimensional Temperature Measurements in Flames Using Filtered Rayleigh Scattering at 254 nm". Appl. Spectrosc. 2008. 62(7): 778-783.
35. J. Kiefer, Z.S. Li, J. Zetterberg, X.S. Bai, M. Aldén. "Investigation of Local Flame Structures and Statistics in Partially Premixed Turbulent Jet Flames Using Simultaneous Single-Shot CH and OH Planar Laser-Induced Fluorescence Imaging". Combust. Flame. 2008. 154(4): 802-818.
36. J. Kiefer, Z.S. Li, T. Seeger, A. Leipertz, M. Aldén. "Planar Laser-Induced Fluorescence of HCO for Instantaneous Flame Front Imaging in Hydrocarbon Flames". Proc. Combust. Inst. 2009. 32(1): 921-928.
37. Z.S. Li, J. Kiefer, J. Zetterberg, M. Linvin, A. Leipertz, X.S. Bai, M. Aldén. "Development of Improved PLIF CH Detection Using an Alexandrite Laser for Single-Shot Investigation of Turbulent and Lean Flames". Proc. Combust. Inst. 2007. 31(1): 727-735.
38. Z.S. Li, B. Li, Z.W. Sun, X.S. Bai, M. Aldén. "Turbulence and Combustion Interaction: High Resolution Local Flame Front Structure Visualization Using Simultaneous Single-Shot PLIF Imaging of CH, OH, and CH_2O in a Piloted Premixed Jet Flame". Combust. Flame. 2010. 157(6): 1087-1096.
39. J. Kiefer, F. Ossler, Z.S. Li, M. Aldén. "Spectral Interferences from Formaldehyde in CH PLIF Flame Front Imaging with Broadband B–X Excitation". Combust. Flame. 2011. 158(3): 583-585.
40. Z.T. Alwahabi, J. Zetterberg, Z.S. Li, M. Aldén. "High Resolution Polarization Spectroscopy and Laser Induced Fluorescence of CO_2 Around 2 μm". Eur. Phys. J. D. 2007. 42(1): 41-47.
41. R.B. Miles, J. Grinstead. K.R. H., G. Diskin. "The RELIEF Flow Tagging Technique and Its Application in Engine Testing Facilities and for Helium-Air Mixing Studies". Meas. Sci. Technol. 2000. 11(9): 1272-1281.
42. P.S. Julienne. "$^3\Sigma_u^- - {}^3\Sigma_u^+$ Coupling in the O_2 $B^3\Sigma_u^-$ Predissociation". J. Mol. Spectrosc. 1976. 63(1): 60-79.
43. S. Watanabe, H. Fujii, H. Kohguchi, T. Hatano, I. Tokue, K. Yamasaki. "Kinetic Study of Vibrational Energy Transfer from a Wide Range of Vibrational Levels of $O_2(X^3\Sigma^-g, v = 6–12)$ to CF_4". J. Phys. Chem. A. 2008. 112(39): 9290-9295.
44. M. Klatt, I.W.M. Smith, A.C. Symonds, R.P. Tuckett, G.N. Ward. "State-Specific Rate Constants for the Relaxation of $O_2(X^3\Sigma g^-, v = 8–11)$ in Collisions with O_2, N_2, NO_2, CO_2, N_2O, CH_4, and He". J. Chem. Soc. Faraday Trans. 1996. 92(2): 193-199.
45. W.G. Bessler, C. Schulz, V. Sick, J.W. Daily. "A Versatile Modeling Tool for Nitric Oxide LIF Spectra". Paper presented at: Proceedings of the Third Joint Meeting of the U.S. Sections of the Combustion Institute. Chicago, IL; March 16-19, 2003. http://www.lifsim.com.
46. G.P. Smith, D.M. Golden, M. Frenklach, N.W. Moriarty, B. Eiteneer, M. Goldenberg, C.T. Bowman, R.K. Hanson, S. Song, W.C. Gardiner Jr., V.V. Lissianski, Z. Qin. "GRI-Mech Home Page". http://www.me.berkeley.edu/gri_mech/.